

100 Gbit/s WDM transmission at 2 μ m: transmission studies in both low-loss hollow core photonic bandgap fiber and solid core fiber

H. Zhang,^{1,*} N. Kavanagh,¹ Z. Li,² J. Zhao,¹ N. Ye,¹ Y. Chen,² N. V. Wheeler,² J. P. Wooller,² J. R. Hayes,² S. R. Sandoghchi,² F. Poletti,² M. N. Petrovich,² S. U. Alam,² R. Phelan,³ J. O'Carroll,³ B. Kelly,³ L. Gr  ner-Nielsen,⁴ D. J. Richardson,² B. Corbett,¹ and F. C. Garcia Gunning¹

¹Tyndall National Institute, University College Cork, Ireland

²Optoelectronics Research Centre, University of Southampton, Highfield, Southampton, SO17 1BJ, UK

³Eblana Photonics Ltd., Dublin 2, Ireland

⁴OFS Denmark, Priorparken 680, 2605 Br  ndby, Denmark

hongyu.zhang@tyndall.ie

Abstract: We show for the first time 100 Gbit/s total capacity at 2 μ m waveband, using 4×9.3 Gbit/s 4-ASK Fast-OFDM direct modulation and 4×15.7 Gbit/s NRZ-OOK external modulation, spanning a 36.3 nm wide wavelength range. WDM transmission was successfully demonstrated over 1.15 km of low-loss hollow core photonic bandgap fiber (HC-PBGF) and over 1 km of solid core fiber (SCF). We conclude that the OSNR penalty associated with the SCF is minimal, while a ~ 1 -2 dB penalty was observed after the HC-PBGF probably due to mode coupling to higher-order modes.

  2015 Optical Society of America

OCIS codes: (060.5295) Photonic crystal fibers; (060.4230) Multiplexing; (060.2330) Fiber optics communications; (060.2340) Fiber optics components; (230.0230) Optical devices.

References and links

1. A. D. Ellis, D. Rafique, and S. Sygletos, "Capacity in fiber optic communications– the case for a radically new fiber," IEEE Phot. Conference (2011), Arlington, paper TuN1.
2. B. Inan, Y. Jung, V. Sleiffer, M. Kuschnerov, L. Gr  ner-Nielsen, S. Adhikari, S. L. Jansen, D. J. Richardson, S. Alam, B. Spinnler, and N. Hanik, "Low computational complexity mode division multiplexed OFDM transmission over 130 km of few mode fiber," in Proceedings of OFC (2013), Anaheim, paper OW4F.4.
3. A. D. Ellis, "The nonlinear Shannon limit and the need for new fibres," Proc. SPIE **8434**, 84340H (2012).
4. N. Mac Suibh  ne, Z. Li, B. B  uerle, J. Zhao, J. Wooller, S. Alam, F. Poletti, M. Petrovich, A. Heidt, N. Wheeler, N. Baddela, E. R. Numkam Fokoua, I. Giles, D. Giles, R. Phelan, J. O'Carroll, B. Kelly, B. Corbett, D. Murphy, A. D. Ellis, D. J. Richardson, and F. Garcia Gunning, "WDM transmission at 2 μ m over low-loss hollow core photonic bandgap fiber," in Proceedings of OFC (2013), Anaheim, paper OW11.6.
5. M. N. Petrovich, F. Poletti, J. P. Wooller, A. M. Heidt, N. K. Baddela, Z. Li, D. R. Gray, R. Slav  k, F. Parmigiani, N. V. Wheeler, J. R. Hayes, E. Numkam, L. Gr  ner-Nielsen, B. P  lsd  ttir, R. Phelan, B. Kelly, J. O'Carroll, M. Becker, N. MacSuibh  ne, J. Zhao, F. C. Gunning, A. D. Ellis, P. Petropoulos, S. U. Alam, and D. J. Richardson, "Demonstration of amplified data transmission at 2 μ m in a low-loss wide bandwidth hollow core photonic bandgap fiber," Opt. Express **21**(23), 28559–28569 (2013).
6. P. J. Roberts, F. Couny, H. Sabert, B. J. Mangan, D. P. Williams, L. Farr, M. W. Mason, A. Tomlinson, T. A. Birks, J. C. Knight, and P. St. J. Russell, "Ultimate low loss of hollow-core photonic crystal fibres," Opt. Express **13**(1), 236–244 (2005).
7. Y. Chen, N. V. Wheeler, N. Baddela, J. Hayes, S. R. Sandoghchi, E. Numkam Fokoua, M. Li, F. Poletti, M. Petrovich, and D. J. Richardson, "Understanding wavelength scaling in 19-cell core hollow-core photonic bandgap fibers," in Proceedings of OFC (2014), San Francisco, paper M2F.4.
8. F. Poletti, N. V. Wheeler, M. N. Petrovich, N. Baddela, E. Numkam Fokoua, J. R. Hayes, D. R. Gray, Z. Li, R. Slav  k, and D. J. Richardson, "Towards high-capacity fibre-optic communications at the speed of light in vacuum," Nat. Photonics **7**(4), 279–284 (2013).
9. Z. Li, A. M. Heidt, N. Simakov, Y. Jung, J. M. O. Daniel, S. U. Alam, and D. J. Richardson, "Diode-pumped wideband thulium-doped fiber amplifiers for optical communications in the 1800 - 2050 nm window," Opt. Express **21**(22), 26450–26455 (2013).
10. R. Phelan, J. O'Carroll, D. Byrne, C. Herbert, J. Somers, and B. Kelly, "In_{0.75}Ga_{0.25}As/InP multiple quantum well discrete mode laser diode emitting at 2 μ m," IEEE Photon. Technol. Lett. **24**(8), 652–654 (2012).

11. B. Kelly, W. Han, F. Gunning, B. Corbett, R. Phelan, J. O'Carroll, H. Yang, F. H. Peters, X. Wang, N. Nudds, P. O'Brien, N. Ye, and N. MacSuihbne, "Butterfly packaged high-speed and low leakage InGaAs quantum well photodiode for 2000nm wavelength systems," *Electron. Lett.* **49**(4), 281–282 (2013).
12. H. Zhang, Z. Li, N. Kavanagh, J. Zhao, N. Ye, Y. Chen, N. V. Wheeler, J. P. Wooller, J. R. Hayes, S. R. Sandoghchi, F. Poletti, M. N. Petrovich, S. U. Alam, R. Phelan, J. O'Carroll, B. Kelly, D. J. Richardson, B. Corbett, and F. C. Garcia Gunning, "81 Gbit/s WDM transmission at 2 μ m over 1.15 km of low-loss hollow core photonic bandgap fiber," in *Proceedings of ECOC (2014)*, Cannes, paper P.5.20.
13. M. Belal, M. Petrovich, N. Wheeler, J. Wooller, A. Masoudi, F. Poletti, S. Alam, D. Richardson, and T. Newson, "First demonstration of a 2- μ m OTDR and its use in photonic bandgap CO₂ sensing fiber," *IEEE Photon. Technol. Lett.* **26**(9), 889–892 (2014).
14. J. Zhao, S. K. Ibrahim, D. Rafique, P. Gunning, and A. D. Ellis, "Symbol synchronization exploiting the symmetric property in optical fast OFDM," *IEEE Photon. Technol. Lett.* **23**(9), 594–596 (2011).

1. Introduction

One focus of the photonics research community has been the development of next generation transmission systems capable of meeting the ever-increasing demand for high bandwidth Internet traffic. Until four years ago, research mostly concentrated on fiber systems operating over standard single mode fiber (SMF) links at 1.55 μ m, with an emphasis on transmitter and receiver optimization. The use of advanced modulation formats, such as phase-shift keying (PSK), quadrature amplitude modulation (QAM), orthogonal frequency division multiplexing (OFDM), polarization division multiplexing (PDM), etc, together with coherent detection schemes, has been widely investigated in the last decade. However, the fundamental propagation properties of standard SMF will ultimately limit the total capacity [1]. To overcome the limitations of SMF, mode division multiplexing techniques in few-mode fiber transmission systems at 1.55 μ m have recently been demonstrated [2], which largely increases the spectral efficiency, and hence the total capacity.

Hollow core photonic bandgap fiber (HC-PBGF), on the other hand, is another promising candidate, due to the potential significant increase in optical signal-to-noise ratio (OSNR) [3]. Recently, we introduced the concept of shifting the transmission band from the conventional C-band to 2 μ m [4, 5], due to the potential ultra-low loss (\sim 0.1 dB/km) HC-PBGF may provide [6, 7], in addition to its near-vacuum latency and lower nonlinearity when compared to standard SMF [8]. Thulium-doped fiber amplifiers (TDFA) which operate over a wide bandwidth spanning from \sim 1.80 μ m to 2.05 μ m are also available at this waveband [9] and their use in a transmission experiment has been demonstrated [5]. Moreover, the increasing availability of telecommunication-grade optical components at 2 μ m, such as lasers [10], modulators and photo-detectors (PD) [11], are making transmission experiments at 2 μ m practical. We previously presented in [4] that either direct laser modulation, or external modulation can be implemented in the 2 μ m region, and successfully demonstrated the first WDM transmission experiment over 290 m of HC-PBGF. In addition, we recently reported error-free 81 Gbit/s WDM transmission at 2 μ m over 1.15 km of low-loss HC-PBGF [12].

In this paper, we demonstrate, for the first time, WDM transmission at 2 μ m having a total capacity of 100 Gbit/s. The WDM signals were transmitted over either 1.15 km of low-loss HC-PBGF, or 1 km of single mode solid core fiber (SCF) intended for the 2 μ m wavelength range [13], both with error-free performance. This demonstration was achieved by using a newer generation of high performance laser sources, a higher bandwidth photo-detector, and by improving the fiber fabrication process [7]. A total capacity of 100 Gbit/s was achieved by externally modulating four lasers with non-return-to-zero (NRZ) on-off keying (OOK) at 15.7 Gbit/s, and directly modulating four lasers with 4-amplitude shift keying (4-ASK) Fast-OFDM [14], each at 9.3 Gbit/s (excluding 7% FEC overheads), spanning a total optical bandwidth of 36.3 nm.

2. Experimental setup and results

The experimental setup for the WDM transmission system is depicted in Fig. 1. The transmitter consisted of four directly modulated (1967.6, 1977.8, 1986.9, and 1992.5 nm) lasers and another four externally modulated (1995.7, 1998.4, 2001.9, and 2003.9 nm) channels. The lasers used were based on highly strained In_{0.75}Ga_{0.25}As multiple quantum well,

ridge waveguide laser diode structures grown on InP substrates and designed for single mode operation at these wavelengths [10]. In order to directly modulate the lasers at the highest baud rate possible, S_{21} frequency response was analyzed for each laser depending on the bias current. It is clear from Fig. 2(a) that the higher the bias current, the higher the RF bandwidth achieved, with values exceeding 5.1 GHz. However, for direct modulation with amplitude modulation formats, the bias current must remain low (in our case <33 mA) in order to guarantee on-off operation, hence limiting the overall RF bandwidth, and therefore the total baud rate that could be applied. On average, the four lasers used for direct modulation presented 3-dB RF bandwidths of up to 3.8 GHz, as exemplified in Fig. 2(b) (black, dotted).

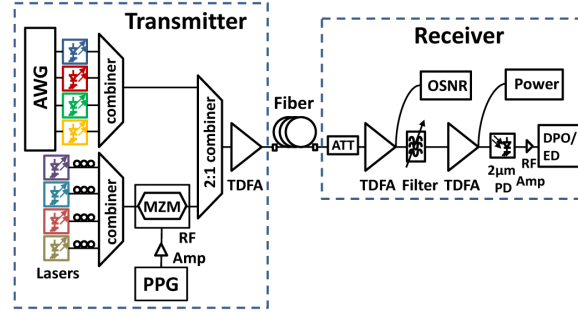


Fig. 1. Experimental setup. AWG: arbitrary waveform generator; MZM: mach-zehnder modulator; PPG: pulse pattern generator; Amp: amplifier; ATT: attenuator; DPO: digital phosphor oscilloscope; ED: error detector.

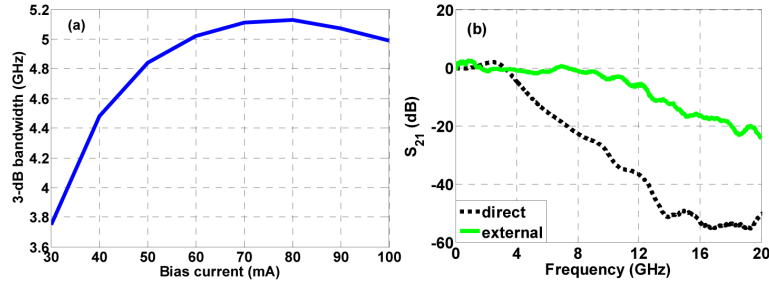


Fig. 2. (a) 3-dB bandwidth vs. bias current for a directly modulated channel 1992.5 nm; (b) S_{21} characterization for: a directly modulated channel at 1992.5 nm at a bias current of 32.5 mA (black, dotted), and an externally modulated channel at 1998.4 nm with a modulator bias of -5.3 V (green, solid), both with a photo-detector at $2 \mu\text{m}$.

Two independent 4-ASK Fast-OFDM signals generated by an AWG each at a DAC rate of 6 GS/s, together with their delayed versions, were used to modulate the four directly modulated lasers. Each Fast-OFDM signal used a 128 discrete cosine transform point size, among which 106 subcarriers were used for data modulation. The optical double side-band 4-ASK Fast-OFDM signal provides a spectral efficiency of 2 bit/s/Hz, so the total data rate per channel was 10 Gbit/s, or 9.3 Gbit/s considering 7% FEC overheads. Each Fast-OFDM frame consisted of one start-of-frame symbol for synchronization [14] and 100 payload symbols.

The other 4 channels were externally modulated using a commercially available LiNbO_3 -based Mach-Zehnder Modulator (MZM) with a V_π of 9.5 V, driven by a $2^{31}-1$ pseudo random bit sequence (PRBS), from a PPG. Polarization controllers (PC) were added after the lasers to align the polarization with the MZM. In this case, we varied the bit rate of the PPG in order to check the performance of the system, with rates of 15.7 Gbit/s, 12.5 Gbit/s and 10 Gbit/s. The overall data rate of these channels was limited by the combined 3-dB RF bandwidth of the MZM and PD of about 10 GHz, as illustrated in Fig. 2(b) (green, solid).

Prior to transmission, a TDFA [9] was used in order to both compensate for the transmitter losses and pre-compensate for the fiber losses. Figure 3(a) illustrates the spectrum of the WDM system after the 1st TDFA (blue dashed curve), with output powers reaching up to 2 dBm/channel. The tilt on the signal corresponds to the roll-off in amplifier gain at longer wavelengths. The lasers clearly have high side-mode suppression ratios, exceeding 40 dB in most cases.

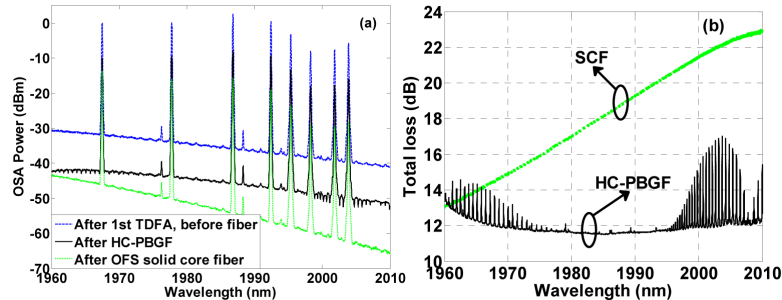


Fig. 3. (a) OSA spectra of (blue, dashed, top) transmitter, (black, solid, middle) after HC-PBGF, and (green, dotted, lowest) after SCF transmission. Narrow dips centered at 1665 and 2004 nm within the black trace are due to CO₂ absorption. (b) Total loss of the HC-PBGF and SCF both including spliced connectorized pigtails. Peaks within the loss spectrum of the HC-PBGF (black, solid) are due to CO₂ absorption. OSA resolution: 0.05 nm.

We used two types of fibers in the experiment: HC-PBGF and SCF. The HC-PBGF used had a 19 cell core design and was 1.15 km long, with a minimum loss of 2.8 dB/km at 1990 nm and a 3-dB bandwidth of 85 nm. The fiber was spliced at both ends to standard SMF; a short length of buffer fiber was used to reduce mode-field mismatch between the SMF and HC-PBGF and thus to enable optimum launch into the fundamental mode. The total insertion loss, including the fiber attenuation and all splice losses, was 11.5 dB at 1987 nm, see Fig. 3(b) (black solid trace), a substantial fraction of which is due to MFD mismatch and is located at the SMF/buffer splice points. Small amounts of carbon dioxide and water vapor were observed to be present in the fiber as a consequence of atmospheric ingress during fiber fabrication. CO₂, in particular, produces bands of discrete loss peaks centered at 1665 and 2004 nm, as shown in Fig. 3(b). It can easily be removed fully by purging the fiber with dry gas. Alternatively, the wavelengths of the WDM channels could also be slightly detuned in order to avoid the gas absorption lines, as we did in the experiment. The full WDM spectrum after HC-PBGF transmission is plotted in Fig. 3(a) (black solid), showing the excess loss of this fiber arrangement, and that the center wavelengths were detuned from CO₂ absorption peaks. The polarization dependent loss of the HC-PBGF remained below 0.3 dB.

The SCF (ClearLite®1700 20 from OFS) is a single mode fiber with a step index design, where the refractive index profile is optimized for application in the 1.7 to 2.1 μm band. It is characterized by a cut off wavelength of 1700 nm. Typical properties at 2.0 μm are: effective area of 55 μm^2 , dispersion of 37 ps/(nm·km) and attenuation of 18 dB/km [13]. The transmission after 1 km of SCF is shown in Fig. 3(b) (green dotted trace), with the additional loss due to the splicing mismatch of the two connectorized pigtails. The additional loss per wavelength is also seen at the WDM spectrum after transmission (Fig. 3(a) – green dotted).

The pre-amplified receiver comprised a variable attenuator placed before the 2nd TDFA, in order to vary the OSNR into the receiver; a commercially available tunable filter with a 3-dB bandwidth of ~ 1.6 nm, sufficient to select each of the WDM channels; and a 3rd TDFA in order to guarantee a constant optical power to the receiver PD for all OSNRs, compensating for the lower gain of the TDFAs between 1990 and 2100 nm. Note that the gains of the 2nd and 3rd TDFAs were ~ 30 dB and ~ 28 dB, respectively. The gain of this 3rd TDFA was adjusted to guarantee a fixed power level of -2 dBm at the PD for all wavelengths. The electrical signal was amplified before a 16 GHz, 100 GS/s digital phosphor oscilloscope (DPO), or an error detector (ED), depending on the channel measured.

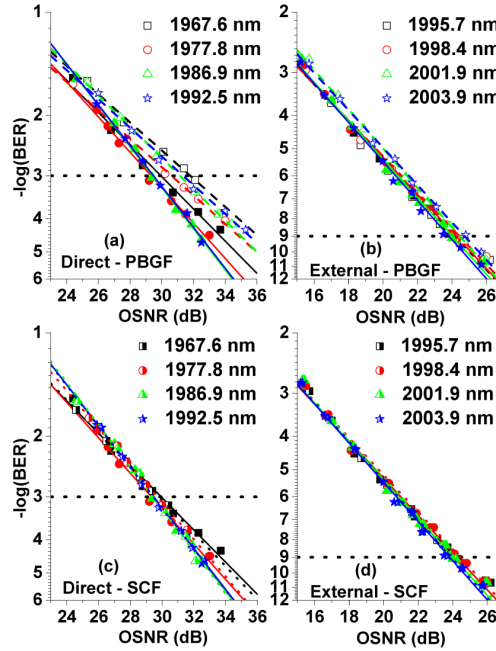


Fig. 4. BER vs. OSNR performance for (a) direct modulation over PBGF, (b) 15.7 Gbit/s external modulation over PBGF, (c) direct modulation over SCF, and (d) 15.7 Gbit/s external modulation over SCF. (In the figures, solid lines – B2B; dashed lines – over PBGF; dotted lines – over SCF.)

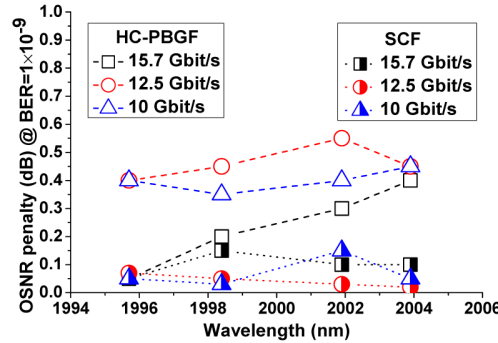


Fig. 5. OSNR penalties at $\text{BER} = 1 \times 10^{-9}$ for externally modulated channels at different bit rates. Note that the dashed and dotted lines are for guidance only.

The performance of the 2 μm WDM system was analyzed in terms of bit error rate (BER) vs. OSNR performance and OSNR penalties after fiber transmission. Note that the OSNR was measured within 0.1 nm bandwidth, and the transmission penalties were calculated at a BER of 1×10^{-3} (FEC limit) for directly modulated channels, and at BER of 1×10^{-9} for externally modulated channels. Figures 4(a) and 4(c) show the performance of the 10 Gbit/s 4-ASK Fast-OFDM channels. The maximum OSNR requirement to achieve a BER of 10^{-3} after transmission was 31.8 dB, with a spread of ~ 1.1 dB between channels. It is observed that the transmission penalties varied from 1.35 to 1.8 dB for HC-PBGF, while for SCF the transmission penalties varied from 0.1 to 0.35 dB only. The spread in required OSNR for the directly modulated channels is probably due to variation in the RF bandwidths of each of the lasers, with lower OSNR requirement for those with larger bandwidths. As the HC-PBGF is not strictly single-mode, it is possible that the additional penalty may be caused by the

asynchronicity between Fast-OFDM symbols, which arises from the modal dispersion and mode coupling to higher-order modes in the HC-PBGF. Figures 4(b) and 4(d) illustrate the performance of all four NRZ-OOK externally modulated channels at a data rate of 15.7 Gbit/s. It can be observed that OSNRs of 24.4 dB or below can be used to achieve a BER of 1×10^{-9} , with a spread of about 0.3 dB between channels. This is most likely due to the amplifier gain tilt as shown in Fig. 3(a).

We also analyzed the externally modulated channels at different data rates, which are shown in Fig. 5. The OSNR penalties are small for all four externally modulated channels at rates of 15.7 Gbit/s (black square), 12.5 Gbit/s (red circle), and 10 Gbit/s (blue triangular), when transmitting over either HC-PBGF or SCF. For example, transmission penalties are no greater than 0.4 dB for HC-PBGF, and 0.1 dB for SCF at a bit rate of 15.7 Gbit/s, with the additional penalty for the HC-PBGF explained as before. Finally, Fig. 6 shows the eye and constellation diagrams for B2B (left) and after transmission (middle and right) for two selected channels. Notice that after 1 km SCF transmission (right), the eye diagram for an externally modulated channel is still very open, and that the constellation diagram for a directly modulated channel is quite clear, indicating no distortion after SCF transmission. The constellation diagram after HC-PBGF transmission however indicates that some distortion is observed for 4-ASK Fast-OFDM signals, as confirmed by the penalties observed in Fig. 4(a).

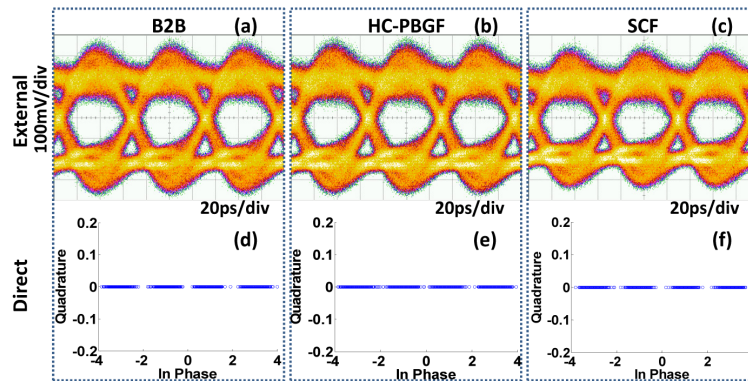


Fig. 6. (top) Eye diagrams of 15.7 Gbit/s NRZ-OOK signal (1998.4 nm) and (bottom) constellation diagrams for 4-ASK Fast-OFDM signal (1992.5 nm), both for (left) B2B, (middle) over HC-PBGF, and (right) over SCF.

3. Conclusion

We have presented eight-channel WDM transmission at 2 μ m over both 1.15 km of low-loss HC-PBGF and 1 km SCF. A 100-Gbit/s transmission system, using 4×9.3 Gbit/s 4-ASK Fast-OFDM directly modulated channels and 4×15.7 Gbit/s NRZ-OOK externally modulated channels, has been demonstrated for the first time, spanning an extended waveband of 36.3 nm. This study illustrates the rapid growth in maturity of technologies for future communication system applications at 2 μ m.

Acknowledgments

The authors would like to acknowledge Phoenix Photonics for supplying some of the passive fiber-based components. This work was funded by the EU 7th Framework Programme under grant agreement 258033 (MODE-GAP) and partially supported by Science Foundation Ireland under 10/CE/I1853 (CTVR-II) and 12/RC/2276 (IPIC). N. Kavanagh would like to thank the support from the Irish Research Council (GOIPG/2014/637).